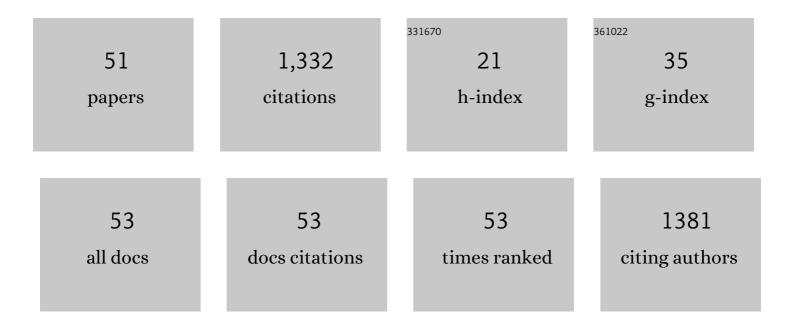
Marianny Y. Combariza

List of Publications by Year in descending order

Source: https://exaly.com/author-pdf/5701515/publications.pdf Version: 2024-02-01



#	Article	IF	CITATIONS
1	Comparative study of Colombian citrus oils by high-resolution gas chromatography and gas chromatography-mass spectrometry. Journal of Chromatography A, 1995, 697, 501-513.	3.7	107
2	Biocomposite of nanostructured MnO2 and fique fibers for efficient dye degradation. Green Chemistry, 2013, 15, 2920.	9.0	87
3	Exploring Occluded Compounds and Their Interactions with Asphaltene Networks Using High-Resolution Mass Spectrometry. Energy & Fuels, 2016, 30, 4550-4561.	5.1	65
4	Volatile secondary metabolites from Spilanthes americana obtained by simultaneous steam distillation-solvent extraction and supercritical fluid extraction. Journal of Chromatography A, 1996, 752, 223-232.	3.7	64
5	Tracing the Compositional Changes of Asphaltenes after Hydroconversion and Thermal Cracking Processes by High-Resolution Mass Spectrometry. Energy & Fuels, 2015, 29, 6330-6341.	5.1	58
6	Gas-phase oon-molecule reactions of transition metal complexes: The effect of different coordination spheres on complex reactivity. Journal of the American Society for Mass Spectrometry, 2002, 13, 813-825.	2.8	57
7	Gas-phase ion–molecule reactions of divalent metal complex ions: Toward coordination structure analysis by mass spectrometry and some intrinsic coordination chemistry along the way. International Journal of Mass Spectrometry, 2005, 244, 109-124.	1.5	49
8	Isolation and characterization of cellulose nanofibrils from Colombian Fique decortication by-products. Carbohydrate Polymers, 2018, 189, 169-177.	10.2	45
9	High Resolution Mass Spectrometric View of Asphaltene–SiO ₂ Interactions. Energy & Fuels, 2015, 29, 1323-1331.	5.1	42
10	Improving compositional space accessibility in (+) APPI FT-ICR mass spectrometric analysis of crude oils by extrography and column chromatography fractionation. Fuel, 2016, 185, 45-58.	6.4	42
11	Exploring the composition of raw and delignified Colombian fique fibers, tow and pulp. Cellulose, 2018, 25, 151-165.	4.9	40
12	Comprehensive Petroporphyrin Identification in Crude Oils Using Highly Selective Electron Transfer Reactions in MALDI-FTICR-MS. Energy & Fuels, 2019, 33, 3899-3907.	5.1	38
13	Effect of Coordination Geometry on the Gas-Phase Reactivity of Four-Coordinate Divalent Metal Ion Complexes. Journal of Physical Chemistry A, 2004, 108, 1757-1763.	2.5	37
14	Correlations between Molecular Composition and Adsorption, Aggregation, and Emulsifying Behaviors of PetroPhase 2017 Asphaltenes and Their Thin-Layer Chromatography Fractions. Energy & Fuels, 2018, 32, 2769-2780.	5.1	35
15	Separation of asphaltene-stabilized water in oil emulsions and immiscible oil/water mixtures using a hydrophobic cellulosic membrane. Fuel, 2018, 231, 297-306.	6.4	32
16	In situ synthesis of gold nanoparticles using fique natural fibers as template. Cellulose, 2012, 19, 1933-1943.	4.9	31
17	Polymeric Inverse Micelles as Selective Peptide Extraction Agents for MALDI-MS Analysis. Analytical Chemistry, 2007, 79, 7124-7130.	6.5	30
18	Selective ionization by electron-transfer MALDI-MS of vanadyl porphyrins from crude oils. Fuel, 2018, 226, 103-111.	6.4	29

#	Article	IF	CITATIONS
19	Controlled synthesis of ZnO particles on the surface of natural cellulosic fibers: effect of concentration, heating and sonication. Cellulose, 2015, 22, 1841-1852.	4.9	26
20	A comparison of the gas, solution, and solid state coordination environments for the Cu(II) complexes of a series of linear aminopyridine ligands with varying ratios of 5- and 6-membered chelate rings. Inorganica Chimica Acta, 2004, 357, 1141-1151.	2.4	24
21	Nanocellulose as an inhibitor of water-in-crude oil emulsion formation. Fuel, 2020, 264, 116830.	6.4	24
22	Influence of post-oxidation reactions on the physicochemical properties of TEMPO-oxidized cellulose nanofibers before and after amidation. Cellulose, 2020, 27, 1273-1288.	4.9	23
23	Advances and Challenges in the Molecular Characterization of Petroporphyrins. Energy & Fuels, 2021, 35, 18056-18077.	5.1	23
24	Facile cellulose nanofibrils amidation using a â€~one-pot' approach. Cellulose, 2017, 24, 717-730.	4.9	22
25	Limonene concentration in lemon (Citrus volkameriana) peel oil as a function of ripeness. Journal of High Resolution Chromatography, 1994, 17, 643-646.	1.4	21
26	Molecular characterization of naphthenic acids from heavy crude oils using MALDI FT-ICR mass spectrometry. Fuel, 2018, 231, 126-133.	6.4	21
27	Influence of nutritional and physicochemical variables on PHB production from raw glycerol obtained from a Colombian biodiesel plant by a wild-type Bacillus megaterium strain. New Biotechnology, 2015, 32, 682-689.	4.4	20
28	Electron-Transfer Ionization of Nanoparticles, Polymers, Porphyrins, and Fullerenes Using Synthetically Tunable α-Cyanophenylenevinylenes as UV MALDI-MS Matrices. ACS Applied Materials & Interfaces, 2019, 11, 10975-10987.	8.0	20
29	The utility of ion–molecule reactions in a quadrupole ion trap mass spectrometer for analyzing metal complex coordination structure. Analytica Chimica Acta, 2003, 496, 233-248.	5.4	19
30	Analysis of naphthenic acids by matrix assisted laser desorption ionization time of flight mass spectrometry. Fuel, 2017, 193, 168-177.	6.4	19
31	A comparison of the gas, solution, and solid state coordination environments for the Ni(II) complexes of a series of linear penta- and hexadentate aminopyridine ligands with accessible Ni(III) oxidation states. Inorganica Chimica Acta, 2004, 357, 51-58.	2.4	17
32	Are Gas-Phase Reactions of Five-Coordinate Divalent Metal Ion Complexes Affected by Coordination Geometry?. Inorganic Chemistry, 2004, 43, 2745-2753.	4.0	17
33	Amidated Cellulose Nanofibrils as Demulsifying Agents for a Natural Water-in-Heavy-Crude-Oil Emulsion. Energy & Fuels, 2020, 34, 14012-14022.	5.1	17
34	Gas-phase reactions of divalent Ni complex ions with acetonitrile: Chelate ring size, inductive, and steric effects. Journal of the American Society for Mass Spectrometry, 2004, 15, 1128-1135.	2.8	16
35	Perspectives in Nanocellulose for Crude Oil Recovery: A Minireview. Energy & Fuels, 2021, 35, 15381-15397.	5.1	14
36	Oligo p-Phenylenevinylene Derivatives as Electron Transfer Matrices for UV-MALDI. Journal of the American Society for Mass Spectrometry, 2017, 28, 2548-2560.	2.8	13

MARIANNY Y. COMBARIZA

#	Article	IF	CITATIONS
37	Enhancement of PHA Production by a Mixed Microbial Culture Using VFA Obtained from the Fermentation of Wastewater from Yeast Industry. Fermentation, 2022, 8, 180.	3.0	12
38	Comparative study of colombian rue oils by high resolution gas chromatography using different detection systems. Journal of Separation Science, 1995, 7, 117-122.	1.0	10
39	Spontaneous assembly of a hydrogen-bonded tetrahedron. Chemical Communications, 2002, , 2260-2261.	4.1	9
40	Synthesis of cellulose nanofiber hydrogels from fique tow and Ag nanoparticles. Cellulose, 2020, 27, 9947-9961.	4.9	9
41	Cellulose biosynthesis using simple sugars available in residual cacao mucilage exudate. Carbohydrate Polymers, 2021, 274, 118645.	10.2	9
42	Asphaltene Structure Modifiers as a Novel Approach for Viscosity Reduction in Heavy Crude Oils. Energy & Fuels, 2020, 34, 5251-5257.	5.1	7
43	Laser desorption ionization and collision induced dissociastion as powerful tools for FT-ICR mass spectrometric characterization of asphaltene fractions enriched in island and archipelago motifs. Fuel, 2022, 323, 124418.	6.4	6
44	Molecular grafting of nanoparticles onto sisal fibers - adhesion to cementitious matrices and novel functionalities. Journal of Molecular Structure, 2021, 1234, 130171.	3.6	5
45	Mass Balance and Compositional Analysis of Biomass Outputs from Cacao Fruits. Molecules, 2022, 27, 3717.	3.8	5
46	Serjanic Acid Improves Immunometabolic Markers in a Diet-Induced Obesity Mouse Model. Molecules, 2020, 25, 1486.	3.8	4
47	Pentacyclic Triterpene Profile and Its Biosynthetic Pathway in Cecropia telenitida as a Prospective Dietary Supplement. Molecules, 2021, 26, 1064.	3.8	4
48	Effect of the Ionization Source on the Targeted Analysis of Nickel and Vanadyl Porphyrins in Crude Oil. Energy & Fuels, 2021, 35, 14542-14552.	5.1	4
49	Magnetic and electrochemical properties of corner-like and grid-like complexes resulting from the self-assembly of two structurally related bis(hydrazones) and iron (II). Inorganica Chimica Acta, 2021, 526, 120514.	2.4	2
50	A mathematical model for polyhydroxybutyrate production by a wild type Bacillus megaterium using raw glycerol from biodiesel industry as sole carbon source. New Biotechnology, 2014, 31, S176.	4.4	1
51	Synthesis, characterization, and redox potential properties of a new double-stranded Ni-bis(hydrazone)-based helicate. Journal of Solid State Chemistry, 2020, 292, 121692.	2.9	1